Crystallographic and Spectroscopic Characterization of a Nonheme Fe(IV)=O Complex

Jan-Uwe Rohde,[1]* Jun-Hee In,[1,2]* Mi Hee Lim,[1,2] William W. Brennessel,[1] Michael R. Bukowski,[1] Audria Stubna,[3] Eckard Münck,[3]† Wonwoo Nam,[2]† Lawrence Que Jr.[1]†

Following the heme paradigm, it is often proposed that dioxygen activation by nonheme monoiron enzymes involves an iron(IV)=oxo intermediate that is responsible for the substrate oxidation step. Such a transient species has now been obtained from a synthetic complex with a nonheme macrocyclic ligand and characterized spectroscopically. Its high-resolution crystal structure reveals an iron-oxygen bond length of 1.646(3) angstroms, demonstrating that a terminal iron(IV)=oxo unit can exist in a nonporphyrin ligand environment and lending credence to proposed mechanisms of nonheme iron catalysis.

High-valent iron-oxo intermediates are frequently invoked in the catalytic cycles of mononuclear iron enzymes that activate O_2 to effect metabolically important oxidative transformations. Such species have been characterized for heme enzymes such as cytochrome P450 (*1*, *2*) and peroxidases (referred to as compounds I and II) (*3*), and corresponding biomimetic oxoiron(IV) porphyrin complexes have greatly contributed to the understanding of their structural, spectroscopic, and reactivity properties (*4*, *5*). This heme paradigm is typically extended to mechanisms proposed for nonheme monoiron enzymes that require pterin or α-ketoglutarate cofactors (*6*, *7*), but evidence for the analogous high-valent iron-oxo species is at best only indirect. In the biomimetic field, there is only one report to date of a mononuclear nonheme Fe(IV)-oxo species, postulated to be $[Fe(IV)(O)(cyclam\text{-}acetate)]^+$ [cyclam-acetate, 1-(carboxymethyl)-1,4,8,11-tetraazacyclotetradecane] from the reaction of the corresponding Fe(II) complex and ozone at –80°C (*8*), but it represented at most 23% of the Fe in the sample and was only characterized by its green color ($\lambda_{max} \sim 676$ nm) and Mössbauer spectra. We now report the high-yield generation of a mononuclear nonheme complex with a terminal Fe(IV)=O unit and describe its spectroscopic properties and high-resolution crystal structure.

The reaction of $[Fe(II)(TMC)(OTf)_2]$ (**1**) [TMC, 1,4,8,11-tetramethyl-1,4,8,11-tetraazacyclotetradecane; OTf, CF_3SO_3] with iodosylbenzene (PhIO) in CH_3CN at –40°C produces within 2 min a pale green intermediate **2** with an absorption maximum wavelength λ_{max} at 820 nm ($\varepsilon = 400\ M^{-1}\ cm^{-1}$) (Fig. 1A) (*9*). Titration experiments show that **2** is formed at greater than 90% yield with 1 equivalent (equiv) PhIO (Fig. 1B). The same species can be obtained in comparable yield upon treatment of **1** with 3 equiv H_2O_2, but its formation takes about 3 hours. Intermediate **2** is stable for at least 1 month at –40°C in acetonitrile but decays upon warming or addition of triphenylphosphane (PPh_3). Similar to [Fe(IV)(O)(TPP)] [TPP, *meso*-tetraphenylporphinato dianion] (*10*), **2** reacts with PPh_3 to form $OPPh_3$, regenerating **1** in the process.

Complex **2** exhibits in zero applied field a Mössbauer spectrum consisting of a doublet (Fig. 2A) with an isomer shift (δ) of 0.17(1) mm/s and a quadrupole splitting (ΔE_Q) of 1.24(1) mm/mm/s. Mössbauer spectra recorded in strong applied fields (B = 0 to 6.5 T) between 4.2 and 100 K show that **2** has integer electronic spin. Spectral simulations using an $S = 1$ spin Hamiltonian yield a parameter set (see legend of Fig. 2) that compares well with those of $S = 1$ Fe(IV)=O complexes [$-A_{iso}$ = 18 to 25 MHz; D = 20 to 37 cm^{-1} (*8*, *11*, *12*)], strongly implicating that **2** is also an $S = 1$ Fe(IV)=O complex (*13*, *14*).

The electrospray mass spectrum of **2** exhibits two prominent ions at a mass-to-charge ratio (m/z) of 184.4 and 476.9, with mass and isotope distribution patterns corresponding to $[Fe(IV)(O)(TMC)(NCCH_3)]^{2+}$ (calculated m/z of 184.5) and $[Fe(IV)(O)(TMC)(OTf)]^+$ (calculated m/z of 477), respectively (Fig. 3). These features upshift accordingly upon introduction of ^{18}O when PhIO pre-equilibrated with $H_2{}^{18}O$ is used to make **2**; furthermore, they disappear when **2** reacts with PPh_3. Taken together, the spectroscopic data provide strong evidence that **2** is $[Fe(IV)(O)(TMC)(NCCH_3)]^{2+}$ (*15*).

Single crystals of **2** derived from the reaction of **1** and H_2O_2 were grown from CH_3CN/diethyl ether at –40°C, and a crystallographic analysis confirmed **2** as

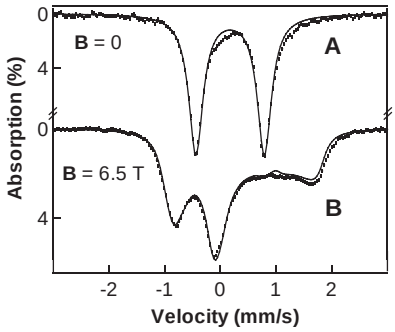

Fig. 2. The 4.2 K Mössbauer spectra of **2** (derived from the reaction of **1** with 3 equiv H_2O_2) in acetonitrile recorded in (**A**) zero field and (**B**) a parallel field of 6.5 T. The data set (10 spectra) was fitted (solid lines) with the $S = 1$ spin Hamiltonian

$$\mathcal{H} = D\left[\hat{S}_z^2 - \frac{1}{3}S(S+1)\right] + E(\hat{S}_x^2 - \hat{S}_y^2) + \beta\hat{\mathbf{S}}\cdot\mathbf{g}\cdot\mathbf{B} + \hat{\mathbf{S}}\cdot\mathbf{A}\cdot\hat{\mathbf{I}} - g_n\beta_n\hat{\mathbf{I}}\cdot\mathbf{B} + H_Q$$

to obtain the following parameters: D = 29(3) cm^{-1}; E/D = 0 (≤0.2); g_x, g_y, g_z [2.3, 2.3, 2]; A_x, A_y, A_z in MHz [–31(4), –25(4), –4(3)]; ΔE_Q = 1.24(1) mm/s; η = 0.5 ($0 \le \eta \le 0.6$); δ = 0.17(1) mm/s (relative to Fe metal). The g values were fixed by the relation $g_{x,y} = 2.0 + 4D/\xi$, where ξ is the single-electron spin-orbit coupling constant (*40*). The sample contained a high-spin Fe(III) contaminant (18% of Fe) that contributes the shoulder at ~0 mm/s in (A); under the conditions of (B), its absorption is essentially outside the chosen velocity range.

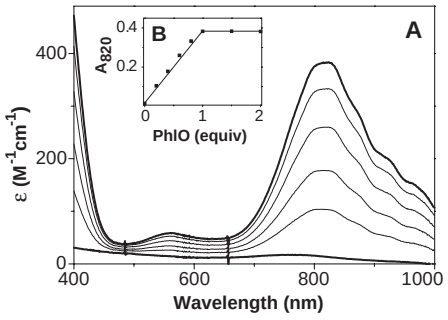

Fig. 1. (**A**) Generation of **2** from **1** by addition of PhIO in increments of 0.2 equiv as monitored by ultraviolet/visible spectroscopy. (**B**) Absorption at 820 nm as a function of number of PhIO equivalents.

[1]Department of Chemistry and Center for Metals in Biocatalysis, University of Minnesota, 207 Pleasant Street SE, Minneapolis, MN 55455, USA. [2]Department of Chemistry and Division of Molecular Life Sciences, Ewha Womans University, Seoul 120-750, Korea. [3]Department of Chemistry, Carnegie Mellon University, Pittsburgh, PA 15213, USA.

*These authors contributed equally to this work.
†To whom correspondence should be addressed. E-mail: emunck@cmu.edu (E.M.); wwnam@ewha.ac.kr (W.N.); que@chem.umn.edu (L.Q.)

$[Fe(O)(TMC)(NCCH_3)](OTf)_2$ (Fig. 4) (*16*). The Fe–O distance (r_{Fe-O}) is 1.646(3) Å, a value that closely matches r_{Fe-O} deduced from extended x-ray absorption fine structure (EXAFS) spectroscopic analysis of oxo-iron(IV) units in synthetic porphyrin complexes (1.62 to 1.67 Å) (*17*, *18*) and heme peroxidase compounds I and II (1.60–1.69 Å) (*17*, *19*). To date, the only reported crystallographic information on complexes with terminal Fe(IV)-oxo units derives from heme protein structures (*20*), namely, those of cytochrome c peroxidase (2.2 to 2.5 Å resolution, r_{Fe-O} ~1.7 to 1.9 Å) (*21*, *22*) and cytochrome P450 (1.9 Å resolution, r_{Fe-O} ~1.65 Å) (*1*), the r_{Fe-O} values of which are necessarily of lower precision than that for **2**.

The 1.646(3) Å distance observed for **2** reflects the tetravalent state of the Fe, the presence of the terminal (as opposed to bridging) oxo ligand, and consequent increased Fe–O π bonding. It is much shorter than the 1.813(3) Å terminal Fe–O distance for the Fe(III) complex $[Fe(III)(O)(L)]^{2-}$ {L, tris[(*N′-tert*-butylureaylato)-*N*-ethyl]amine trianion} (*23*) and the 1.79 Å distance associated with the Fe–O bonds in the di-oxo-bridged $[Fe(IV)_2(\mu\text{-}O)_2(BPMCN)_2]^{4+}$ [BPMCN, *N,N′*-bis(2-pyridylmethyl)-*N,N′*-dimethyl-*trans*-1,2-diaminocyclohexane] (*24*), but is comparable to the 1.666(2) Å average terminal Fe–O distance in $K_2Fe(VI)O_4$ (*25*).

The TMC ligand coordinates to the metal center in the plane (rms deviation of 0.0039 Å) perpendicular to the Fe–O axis, with the Fe atom slightly out of the plane defined by N1, N2, N3, and N4 toward the acetonitrile ligand by 0.0324(16) Å; all four *N*-methyl groups point away from the oxo ligand below this plane. The $Fe-N_{TMC}$ bonds range from 2.067(3) to 2.117(3) Å and average 2.091 Å, comparable to the $Fe-N_{amine}$ bonds [2.049(3) Å] of $[Fe(III)Fe(IV)(\mu\text{-}O)_2(5\text{-}Et_3\text{-}TPA)_2](ClO_4)_3$ [5-Et_3-TPA, tris(5-ethylpyridyl-2-methyl)amine] (*26*). The Fe–N5 bond [2.058(3) Å] of the sixth ligand, CH_3CN, is nearly collinear with the Fe=O bond [∠O1–Fe–N5 178.89(13)°]. As illustrated by the space-filling model in Fig. 4B, the oxo ligand is nestled in a bed of H atoms from C–H bonds of the macrocyclic ligand. The restricted access to the oxo group by external substrates may explain the stability of **2**. Its self-destruction may be inhibited by the nearly perpendicular disposition of the six C–H bonds proximal to the oxo atom relative to corresponding O–H vectors; the $O_{oxo} \cdots H$–C angles average 105°, which is significantly different from the linear $O_{oxo} \cdots H$–C configuration favored by density functional theory calculations as the ideal geometry for H-atom abstraction by a high-valent iron-oxo moiety (*27*–*30*).

The isolation of a nonheme complex with a terminal Fe(IV)=O unit has allowed us to determine its properties in the absence of other chromophores. In particular, **2** exhibits a near-infrared transition that may be characteristic of such units. We have attempted to probe this transition using 752.5-nm laser excitation to obtain Raman vibrations of **2** that may be in resonance with this band, but no enhanced vibration of the Fe=O unit could be detected, perhaps attributable to the low intensity of this absorption band. This band may be too weak to be assigned as an oxo-to-Fe(IV) charge transfer transition and may instead arise mainly from a *d-d* transition, but more detailed spectroscopic studies are required for a definitive assignment. The Fe(IV)=O stretch of **2** can, however, be observed at 834 cm^{-1} in Fourier transform infrared experiments. This value falls within the range of values found for corresponding Fe(IV)=O units with heme ligands (*31*) and downshifts by 34 cm^{-1} in the ^{18}O isotopomer, as expected for an Fe-O diatomic vibration.

We have thus isolated and characterized a nonheme complex with a terminal Fe(IV)=O unit. However, in finding a ligand environment that increases the lifetime of the Fe(IV)=O moiety and allows crystallization of the complex, we have greatly tempered its oxidative reactivity. In contrast, the Fe(II) complex of the parent cyclam (1,4,8,11-tetraazacyclotetradecane) ligand is an effective catalyst for olefin epoxidation with H_2O_2 as oxidant (*32*) and the postulated $[Fe(IV)(O)(cyclam\text{-}acetate)]^+$ decays within minutes at −40°C (*8*). Moreover, indirect evidence for more reactive Fe(IV)=O species has been found in the reactions of related Fe(TPA) complexes [TPA, tris(2-pyridylmethyl) amine] with ROOH (*33*, *34*), wherein the putative Fe(IV)=O species effects sulfoxidation, alcohol oxidation, and arene hydroxylation. It should thus be possible to design ligands that allow the Fe(IV)=O unit to be observed spectroscopically, and at the same time exhibit greater oxidative capabilities than found for **2**. The present work provides the synthetic precedent for invoking such high-valent species in the catalytic cycles of nonheme monoiron enzymes that activate O_2.

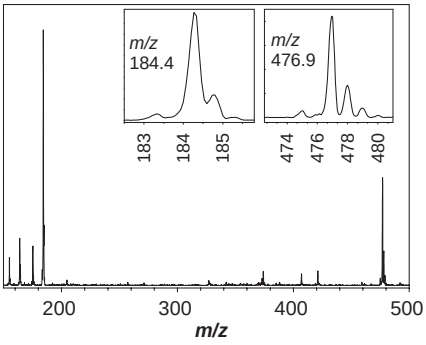

Fig. 3. Electrospray mass spectrum of **2**. Two prominent features at *m/z* of 184.4 and 476.9 correspond to $[Fe(IV)(O)(TMC)(NCCH_3)]^{2+}$ and $[Fe(IV)(O)(TMC)(OTf)]^+$, respectively. Insets show the observed isotope distribution patterns for ions at *m/z* of 184.4 and 476.9.

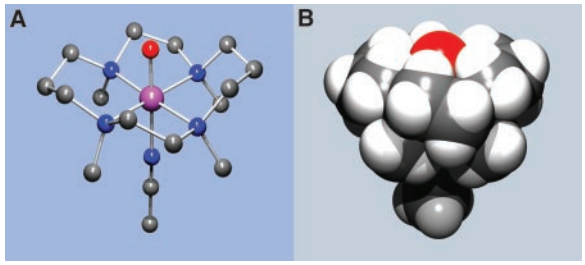

Fig. 4. (**A**) Molecular structure of the cation of *trans*-$[Fe(IV)(O)(TMC)(NCCH_3)](OTf)_2$ (**2**) and (**B**) space-filling representation, derived from the high-resolution single-crystal structure determination. Selected bond lengths (Å): Fe–O, 1.646(3); $Fe-N_{TMC}$, 2.067(3), 2.069(3), 2.109(3), 2.117(3); $Fe-N_{acetonitrile}$, 2.058(3). The crystallographic data have been deposited with the Cambridge Crystallographic Data Centre (*41*) under CCDC 192768.

References and Notes

1. I. Schlichting *et al.*, *Science* **287**, 1615 (2000).
2. D. G. Kellner, S.-C. Hung, K. E. Weiss, S. G. Sligar, *J. Biol. Chem.* **277**, 9641 (2002).
3. M. Sono, M. P. Roach, E. D. Coulter, J. H. Dawson, *Chem. Rev.* **96**, 2841 (1996).
4. J. T. Groves, Y.-Z. Han, in *Cytochrome P450: Structure, Mechanism, and Biochemistry*, P. R. Ortiz de Montellano, Ed. (Plenum, New York, 1995), pp. 3–48.
5. Y. Watanabe, H. Fujii, *Struct. Bonding* **97**, 61 (2000).
6. L. Que Jr., R. Y. N. Ho, *Chem. Rev.* **96**, 2607 (1996).
7. E. I. Solomon *et al.*, *Chem. Rev.* **100**, 235 (2000).
8. C. A. Grapperhaus, B. Mienert, E. Bill, T. Weyhermüller, K. Wieghardt, *Inorg. Chem.* **39**, 5306 (2000).
9. Materials and methods are available as supporting material on *Science* Online.
10. D.-H. Chin, A. L. Balch, G. N. La Mar, *J. Am. Chem. Soc.* **102**, 5945 (1980).
11. P. G. Debrunner, in *Iron Porphyrins*, A. B. P. Lever, H. B. Gray, Eds. (VCH, New York, 1989), vol. III, p. 199.
12. V. Schünemann *et al.*, *FEBS Lett.* **479**, 149 (2000).
13. The δ value of **2** is somewhat greater than those of other Fe(IV) complexes reported to date (range 0.01 to 0.14 mm/s), but our ongoing study of related Fe(IV) complexes shows that δ increases with the number of tertiary amine ligands.
14. Fits to an $S = 2$ Fe(IV) site required $D = 25\ cm^{-1}$ and $A_{iso} = (A_x + A_y + A_z)/3 = -7$ MHz. This A_{iso} is at least three times smaller than those observed for $S = 2$ Fe(IV) sites [–21.7 MHz to –25.3 MHz (*35*–*37*)]. Because the magnetic hyperfine field at 100 K is proportional to $S(S+1)$ and **A**, choice of the wrong spin, namely $S = 2$, results in an unreasonably small A_{iso}.
15. A bis(μ-oxo)diiron(IV) complex has also been reported by Costas *et al.* (*24*) with quite distinct properties.
16. The structure of the Ru(IV) analog $[Ru(IV)(O)(TMC)(NCCH_3)](PF_6)_2$ was reported by Che *et al.* (*38*).
17. J. E. Penner-Hahn *et al.*, *J. Am. Chem. Soc.* **108**, 7819 (1986).
18. T. Wolter *et al.*, *J. Inorg. Biochem.* **78**, 117 (2000).
19. M. Chance, L. Powers, C. Kumar, B. Chance, *Biochemistry* **25**, 1266 (1986).

20. The crystal structure of an Fe(IV)(O)(porphyrin) complex with an Fe–O bond length of 1.604 Å was briefly mentioned in a footnote of Schappacher *et al.* (*39*), but this result has not been subsequently presented in greater detail.
21. S. L. Edwards, N. H. Xuong, R. C. Hamlin, J. Kraut, *Biochemistry* **26**, 1503 (1987).
22. V. Fülöp *et al.*, *Structure* **2**, 210 (1994).
23. C. E. MacBeth *et al.*, *Science* **289**, 938 (2000).
24. M. Costas *et al.*, *J. Am. Chem. Soc.* **123**, 12931 (2001).
25. M. L. Hopper, E. O. Schlemper, R. K. Murmann, *Acta Crystallogr. B* **38**, 2237 (1982).
26. H.-F. Hsu, Y. Dong, L. Shu, V. G. Young Jr., L. Que Jr., *J. Am. Chem. Soc.* **121**, 5230 (1999).
27. F. Ogliaro *et al.*, *J. Am. Chem. Soc.* **122**, 8977 (2000).
28. M. Hata, Y. Hirano, T. Hoshino, M. Tsuda, *J. Am. Chem. Soc.* **123**, 6410 (2001).
29. P. E. M. Siegbahn, *J. Biol. Inorg. Chem.* **6**, 27 (2001).
30. H. Basch, K. Mogi, D. G. Musaev, K. Morokuma, *J. Am. Chem. Soc.* **121**, 7249 (1999).
31. T. Kitagawa, Y. Mizutani, *Coord. Chem. Rev.* **135/136**, 685 (1994).
32. W. Nam, R. Y. N. Ho, J. S. Valentine, *J. Am. Chem. Soc.* **113**, 7052 (1991).
33. S. J. Lange, H. Miyake, L. Que Jr., *J. Am. Chem. Soc.* **121**, 6330 (1999).
34. H. Miyake, K. Chen, S. J. Lange, L. Que Jr., *Inorg. Chem.* **40**, 3534 (2001).
35. K. L. Kostka *et al.*, *J. Am. Chem. Soc.* **115**, 6746 (1993).
36. H. Zheng, S. J. Yoo, E. Münck, L. Que Jr., *J. Am. Chem. Soc.* **122**, 3789 (2000).
37. D. Lee *et al.*, *J. Am. Chem. Soc.* **124**, 3993 (2002).
38. C.-M. Che, K.-Y. Wong, T. C. W. Mak, *J. Chem. Soc. Chem. Commun.* **1985**, 546 (1985).
39. M. Schappacher, R. Weiss, R. Montiel-Montoya, A. Trautwein, A. Tabard, *J. Am. Chem. Soc.* **107**, 3736 (1985).
40. W. T. Oosterhuis, G. Lang, *J. Chem. Phys.* **58**, 4757 (1973).
41. Copies of the data can be obtained free of charge via www.ccdc.cam.ac.uk/conts/retrieving.html (or from the CCDC, 12 Union Road, Cambridge CB2 1EZ, UK).
42. Supported by grants from NIH (GM-33162 and GM-38767 to L.Q. and GM-22701 to E.M.) and the Korea Science and Engineering Foundation (KOSEF) (R02-2002-000-00048-0 to W.N.), a postdoctoral fellowship from the Deutsche Forschungsgemeinschaft (J.-U.R.), and a graduate fellowship from NSF (A.S.). We also thank KOSEF and NSF for stimulating this international cooperative research effort.

Supporting Online Material

www.sciencemag.org/cgi/content/full/299/5609/1037/DC1
Materials and Methods
Fig. S1
Table S1
References

9 September 2002; accepted 10 December 2002

Crystal Structure of Naphthalene Dioxygenase: Side-on Binding of Dioxygen to Iron

Andreas Karlsson,[1] Juanito V. Parales,[2] Rebecca E. Parales,[2] David T. Gibson,[2] Hans Eklund,[1] S. Ramaswamy[3]*

Binding of oxygen to iron is exploited in several biological and chemical processes. Although computational and spectroscopic results have suggested side-on binding, only end-on binding of oxygen to iron has been observed in crystal structures. We have determined structures of naphthalene dioxygenase that show a molecular oxygen species bound to the mononuclear iron in a side-on fashion. In a complex with substrate and dioxygen, the dioxygen molecule is lined up for an attack on the double bond of the aromatic substrate. The structures reported here provide the basis for a reaction mechanism and for the high stereospecificity of the reaction catalyzed by naphthalene dioxygenase.

Oxygenases that catalyze the addition of molecular oxygen to organic substrates play a pivotal role in diverse areas such as drug metabolism and the biodegradation of environmental pollutants. Oxygen activation by cytochrome(s) P450 (*1–6*) and diiron enzymes such as methane monooxygenase (MMO) (*7–10*) have been studied in detail. In contrast, less is known about bacterial Rieske non-heme iron dioxygenases (RDOs) that catalyze the stereospecific addition of dioxygen to aromatic hydrocarbons (*11*). The reaction products are chiral arene *cis*-dihydrodiols that are of current interest in enantioselective synthesis (*12*).

Naphthalene dioxygenase (NDO) from *Pseudomonas* sp., the only RDO for which a crystal structure is known (*13*), oxidizes naphthalene to *cis*-(1*R*,2*S*)-dihydroxy-1,2-dihydronaphthalene (*14*). The enzyme has an $\alpha_3\beta_3$ composition, and each α subunit contains a Rieske [2Fe-2S] center and mononuclear iron at the active site. Electrons from the reduced form of nicotinamide adenine dinucleotide (NADH) are transferred to NDO via an iron-sulfur flavoprotein (*15*) and a Rieske ferredoxin (*16*). The subsequent steps lead to oxygen activation and the formation of naphthalene *cis*-dihydrodiol. Although several hypotheses have been advanced to account for oxygen activation and catalysis by RDOs, the reaction mechanism remains elusive (*17–21*). To understand the molecular basis for the reaction, we have formed complexes of NDO with substrates, oxygen, substrate plus oxygen, and product and have determined their structures by x-ray crystallography (Table 1).

Substrate binding was achieved by soaking crystals of NDO in ethanol solutions of the substrates as described (*22*). Indole (*22*) and naphthalene (Fig. 1A) bind in an elongated cleft, with the carbon atoms to be hydroxylated at a distance of about 4 Å from the ferrous iron at the active site (*22*). The structure, determined from crystals of NDO that were reduced with dithionite and then exposed to oxygen, reveals that dioxygen binds side-on close to the mononuclear iron at the active site (Fig. 1B). The distances between the oxygen atoms and iron are 2.2 and 2.3 Å, respectively. The distance between the oxygen atoms was originally fixed at 1.45 Å during refinement (*23*). The O-O distance, upon crystallographic refinement, converged to 1.4 Å. The refined distance between the oxygen atoms suggests that the structure contains a peroxide species, but the resolution of 1.75 Å does not definitively permit such an assignment. Nor do available spectroscopic studies give a reliable conclusion. Electron paramagnetic resonance (EPR) studies, which were done under different conditions from those of the crystallographic studies, show that a small amount of the mononuclear ferrous iron is oxidized upon exposure to oxygen when oxygen alone is allowed to react with the fully reduced enzyme (*17*). The reaction with oxygen is much faster with substrate present.

In a similar experiment, reduced crystals soaked with indole were exposed to oxygen in a pressure cell at –17°C. The structure obtained from these crystals, besides having indole bound, exhibited clear density for a dioxygen species bound side-on with both oxygens coordinated to the iron (Fig. 1C). The turnover reaction is apparently slow under these conditions because no product was visible in the electron density maps. The refined iron-oxygen distances are 1.8 and 2.0 Å and the refined distance between the oxygen atoms converges to about 1.4 Å. The temperature factors of the two oxygen atoms are higher than those of the surrounding atoms (32 and 39; Fe is 20). The bound substrate also has B-factors comparable to the dioxygen species. This indicates that the substrate and dioxygen species have high but not full occupancy. All attempts to model the structure with one bound oxygen (water/hydroxide) resulted in excess residual electron density (*23*). The structure of the fully oxidized enzyme shows that two water molecules bind differently to the ferric ion in

[1]Department of Molecular Biology, Swedish University of Agricultural Sciences, Box 590, Biomedical Center, 75124 Uppsala, Sweden. [2]Department of Microbiology and Center for Biocatalysis and Bioprocessing, [3]Department of Biochemistry, University of Iowa, Iowa City, IA 52242, USA.

*To whom correspondence should be addressed. E-mail: s-ramaswamy@uiowa.edu